

Sustained RF oscillations from thermally induced spin-transfer torque

David Luc¹ and Xavier Waintal¹

¹CEA-INAC/UJF Grenoble 1, SPSMS UMR-E 9001, Grenoble F-38054, France

(Dated: February 20, 2014)

We investigate the angular dependence of the spin torque generated when applying a temperature difference across a spin-valve. Our study shows the presence of a non-trivial fixed point in this angular dependence, *i.e.* the possibility for a temperature gradient to stabilize radio frequency oscillations without the need for an external magnetic field. This so called "wavy" behavior can already be found upon applying a voltage difference across a spin-valve but we find that this effect is much more pronounced with a temperature difference. Our semi-classical theory is parametrized with experimentally measured parameters and allows one to predict the amplitude of the torque with good precision. Although thermal spin torque is by nature less effective than its voltage counterpart, we find that in certain geometries, temperature differences as low as a few degrees should be sufficient to trigger the switching of the magnetization.

Spin caloritronics[1–7] studies the interplay of charge, spin and heat transport and provides extensions to some of the spintronics concepts. One of interest to us is the spin-transfer torque (STT)[8–10], first predicted by Slonczewski and Berger in 1996[11, 12]. STT is the angular momentum deposited by a spin-polarized current on a ferromagnetic layer. It is at the origin of interesting out of equilibrium dynamics for the magnetization layer leading to magnetic reversal or sustained RF oscillations. The later effect, known as spin-torque oscillator (STO)[13, 14] is a promising candidate for agile RF sources. Although most STO require an external magnetic field, it was also discovered that STT can, in some very asymmetric spin-valves, stabilize an oscillating state in the absence of an external magnetic field. This is the so-called waviness[15–17]. In 2007, in one of the first article on "caloritronics", Bauer *et al.* considered another route for creating STT via the combination of spintronics with thermoelectric effects[2]: the so-called thermal STT. Spin-dependent thermoelectric effects soon started to attract some theoretical and experimental interest [4–6, 18–20]

In this letter, we investigate the angular dependence of the STT induced by temperature gradients applied across various type of magnetic spin valves. Our semi-classical theory, carefully tabulated with experimentally measured parameters, shows that thermally-induced STT is naturally "wavy" for a wide range of devices. By optimizing the geometry of the sample, we predict that magnetic switching can be obtained with temperature differences as low as a few degrees.

Semi-classical drift-diffusion approach. Our starting point is a semi-classical approach for metallic magnetic multilayers that treats the charge degrees of freedom at the drift-diffusion level yet retains all the information about spin degrees of freedom[16, 21]. This approach to which we refer as CRMT[16, 21, 22] (for Continuous Random Matrix Theory) can be seen as a generaliza-

tion of the Valet Fert theory[23] to systems with non collinear magnetization[24]. It is also equivalent to the so-called (Generalized) Circuit Theory[25]. Here we generalize CRMT to include heat flow and thermoelectric effects. In addition to the charge I_α and spin J_α current densities, we therefore add the heat current density Q_α ($\alpha = x, y, z$ being the direction of propagation). Similarly, in addition to the charge μ_c and spin μ potentials, we include the temperature θ (in energy unit, $\theta = k_B T$ where T is the actual temperature). Note that in this letter, we assume that a single temperature can be defined for both majority and minority electrons. Thermoelectric effects are described by spin dependent Seebeck and Peltier coefficients[4, 19, 26, 27]. We note S_\uparrow (S_\downarrow) the spin-dependent Seebeck coefficients for majority (minority) electrons while the Peltier coefficients are given by Onsager relation $\Pi_\sigma = S_\sigma T^*$ where T^* is the average temperature. We further introduce dimensionless Seebeck coefficients in unit of $k_B/e \approx 80 \mu V.K^{-1}$: $s = e(S_\uparrow + S_\downarrow)/(2k_B)$ and $\Delta s = e(S_\uparrow - S_\downarrow)/(2k_B)$ characterize respectively the average and the polarization of the Seebeck effect. Recent experiments provide the first spin resolved values of these quantities for ferromagnetic materials[19]: $s_{Co} \approx -0.25$ and $\Delta s_{Co} \approx -0.02$ for cobalt, and $s_{Py} \approx -0.21$ and $\Delta s_{Py} \approx -0.044$ for permalloy. We introduce reduced currents (with unit of energy) as follows,

$$I_\alpha = 4j_\alpha^c/(e\mathcal{R}_{Sh}) \quad (1)$$

$$J_\alpha = 2\hbar j_\alpha/(e^2\mathcal{R}_{Sh}) \quad (2)$$

$$Q_\alpha = 4k_B T^* j_\alpha^q/(e^2\mathcal{R}_{Sh}) \quad (3)$$

where \mathcal{R}_{Sh} is the Sharvin resistance for a unit surface (with typical value $\mathcal{R}_{Sh} \approx 1 f\Omega.m^2$), and $e < 0$ is the charge of the electron. These variables follow a set of Ohm-like (or Fourier-like) equations,

$$-\ell_* \partial_\alpha \mu_c = j_\alpha^c - \beta \mathbf{j}_\alpha \cdot \mathbf{m} + \frac{\ell_*}{\ell_H} s (s j_\alpha^c + \Delta s \mathbf{j}_\alpha \cdot \mathbf{m}) - \frac{\ell_*}{\ell_H} s j_\alpha^q \quad (4)$$

$$-\ell_* \partial_\alpha \boldsymbol{\mu} = \mathbf{j}_\alpha - \beta j_\alpha^c \mathbf{m} + \frac{\ell_*}{\ell_H} \Delta s (s j_\alpha^c \mathbf{m} + \Delta s \mathbf{j}_\alpha) - \frac{\ell_*}{\ell_H} \Delta s j_\alpha^q \mathbf{m} + \frac{\ell_*}{\ell_\perp} (\mathbf{m} \times \mathbf{j}_\alpha) \times \mathbf{m} - \frac{\ell_*}{\ell_L} (\mathbf{m} \times \mathbf{j}_\alpha) \quad (5)$$

$$-\ell_H \partial_\alpha \theta = -s j_\alpha^c - \Delta s \mathbf{j}_\alpha \cdot \mathbf{m} + j_\alpha^q \quad (6)$$

Eqs(4-6) are the extension of Eqs.(1)-(4) of [24]. The unit vector \mathbf{m} is the local direction of the magnetization (bold vectors correspond to spin space while explicit components $\alpha = x, y, z$ are used for real space). The parameters involved are the mean free paths for the majority (ℓ_\uparrow) and minority (ℓ_\downarrow) electrons, related to the spin-dependent resistivities ρ_σ as $\ell_{\uparrow(\downarrow)} = \mathcal{R}_{\text{Sh}}/\rho_{\uparrow(\downarrow)}$. They can be expressed alternatively in term of ℓ_* , the average mean free path ($1/\ell_* = 1/\ell_\uparrow + 1/\ell_\downarrow$), and $\beta = (\ell_\uparrow - \ell_\downarrow)/(\ell_\uparrow + \ell_\downarrow)$, the asymmetry of the spin resolve asymmetry (with a definition identical to the usual Valet-Fert parameter). Two length scales characterize the behavior of a spin perpendicular to the magnetization: the Larmor precession length ℓ_L and the transverse penetration length ℓ_\perp , see [24]. Finally, ℓ_H is the heat diffusion length. For purely electronic heat transfer Wiedemann-Franz law implies, $\ell_H = \ell_* (\mathcal{L} - s^2 + 2\beta s \Delta s + \Delta s^2)/(1 - \beta^2)$ with $\mathcal{L} = \pi^2/3$. However, to account for the phonon contribution, higher values of \mathcal{L} can be used. A second set of equation expresses the conservation (or lack thereof) of the different currents,

$$\sum_\alpha \partial_\alpha j_\alpha^c = 0 \quad (7)$$

$$\sum_\alpha \partial_\alpha j_\alpha^q = 0 \quad (8)$$

$$\sum_\alpha \partial_\alpha \mathbf{j}_\alpha = -\frac{\ell_*}{\ell_{sf}^2} \boldsymbol{\mu} - \frac{1}{\ell_\perp} (\mathbf{m} \times \boldsymbol{\mu}) \times \mathbf{m} + \frac{1}{\ell_L} (\mathbf{m} \times \boldsymbol{\mu}) \quad (9)$$

where ℓ_{sf} is the spin diffusion length. Similarly, a set of equations describe the interface boundary conditions between a ferromagnet and a normal metal. The charge and spin sectors are described by the usual spin dependent interface resistances r_σ^b , namely Equation (8) and (9) of Ref.[24]. The heat sector is given by (neglecting interface thermoelectric effects),

$$\sum_\alpha n_\alpha j_\alpha^q = \mathcal{L} \frac{\mathcal{R}_{\text{Sh}}}{4r_*^b(1 - \gamma^2)} (\theta_N - \theta_F) \quad (10)$$

Where θ_N and θ_F are the temperatures on both sides of the Ferro-Normal interface and the interface resistances have been parametrized according to the usual Valet-Fert notation $r_{\uparrow,\downarrow}^b = 2r_*^b(1 \pm \gamma)$. n_α are the components of the normal unit vector pointing towards the magnetic

side of the interface. Last, the boundary conditions at the metallic electrodes are given by Eqs.(12) and (13) of Ref.[24] for the spin and charge sector while the heat sector reads (n_α points towards the system),

$$\sum_\alpha n_\alpha j_\alpha^q + \theta = k_B \Delta T \quad (11)$$

where $k_B \Delta T$ is the temperature difference applied to the reservoir with respect to the reference temperature T^* .

Application to thermally induced STT in a spin-valve
Let us now turn to a spin-valve made of the following stack: $\text{Cu}_{20}|\text{Co}_{\text{LCo}}|\text{Cu}_2|\text{Py}_{\text{LPy}}(\varphi)|\text{Cu}_{10}$ where the indices indicate the corresponding thicknesses in nm and φ is the angle of the magnetization of the free (permalloy) layer with respect to the fixed cobalt layer. Following usual practice[11, 21], the torque $\boldsymbol{\tau}$ exerted on the free layer is defined as the difference of spin currents on both side of the layer (spin relaxation only provides extremely small corrections here, see[24]). We used standard material parameters for the mean free paths and spin-diffusion lengths of Cu, Co and Py, as extracted from giant magnetoresistance measurements[24]) while we focus on the values given in Ref[19] for the spin resolved Seebeck coefficients (see supplementary material).

Fig. 1 shows the angular dependence of the spin torque for three different types of setups (see the right part of Fig.2 for a cartoon). In the first, we apply a voltage bias V_b across the spin valve and calculate the torkance $\tau_V = d\tau/dV_b$. We recover the usual feature of STT in metallic spin valve with a stronger torque in the anti-parallel configuration than in the parallel one (black curves). In the second, we apply a temperature difference ΔT across the spin valve in an open circuit configuration so that no current can flow through the device. This is the "pure" spin Seebeck case $\tau_P = d\tau/d\Delta T$ as it is given by spin current only. In the last closed circuit or "mixed" configuration, a temperature difference is applied and a current can flow through the spin valve (i.e. the two electrodes of the spin valve are electrically - but not thermally - short circuited). In this last configuration the Seebeck effect induces a finite current density which in turn induces a STT very similar to the voltage driven one. Hence, one find that the mixed thermal torkance $\tau_M = d\tau/d\Delta T$ is somehow intermediate between the pure and the voltage torkances. The most remarkable feature

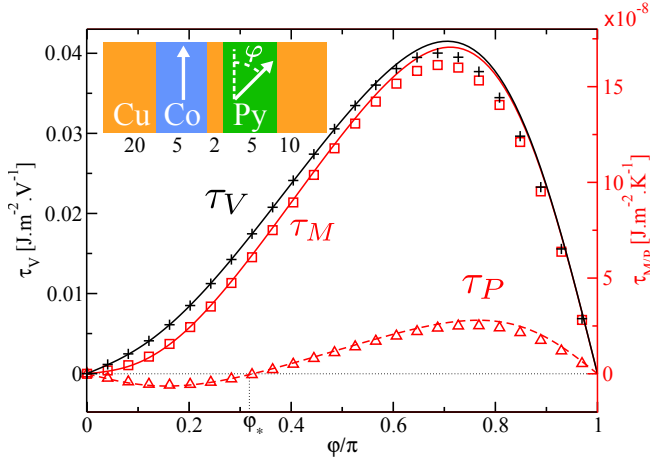


FIG. 1. Spin-transfer torque obtained when applying a voltage (τ_V , bottom curve), a temperature gradient (τ_M , top full curve), and a temperature gradient in the open-circuit configuration (τ_P , top dashed curve), versus the magnetization angle φ of the Py layer with respect to that of the Co layer. Symbols represent the simulations including spin-flip scattering, while lines correspond to the analytical calculation Eq. (18). Here $L_{Co} = L_{Py} = 5$ nm. Inset: sketch of the spin valve.

of Fig. 1 is the appearance in the pure case τ_P of a finite angle $\varphi^* \approx \pi/3$ where τ_P vanishes. Depending on the sign of the thermal gradient, this new fixed point will be stabilized or destabilized. When stabilized, it corresponds to a fast precessional state which forms a STO. In the context of voltage induced torque, these “wavy” structures, which do not require magnetic field in contrast to more conventional STOs, have been discussed for highly asymmetric spin valves[15–17]. Here we find that thermally induce STT corresponds to a wavy angular dependence of the torque in a much broader range of parameters. Fig. 2, shows the “phase diagram” of the spin valve as a function of the thicknesses L_{Co} and L_{Py} of the fixed cobalt and free permalloy layers. The various regions correspond to the presence of a wavy angular dependence of the torque for thermal induced spin torque (P and M) and the standard voltage induced STT (V). The color measures the waviness angle of τ_P , when it exists. This diagram illustrates several points, the first of which is that thermally induced torque is wavy in a much broader range of thicknesses than the voltage induced torque. Second, the various torques behave quite differently. A thicker Co layer is beneficial for the waviness of τ_V , whereas it is detrimental for that of τ_P and τ_M . Also, for the limit of a very thin Co layer, the waviness angle for τ_P comes close to $\pi/2$. As a comparison, the maximum waviness angle in this diagram for τ_V (not represented) is five times lower.

To proceed, we introduce a minimum model to estimate the critical value of the temperature gradient needed to trigger magnetic switching or STO behavior. In the macrospin approximation in presence of a purely

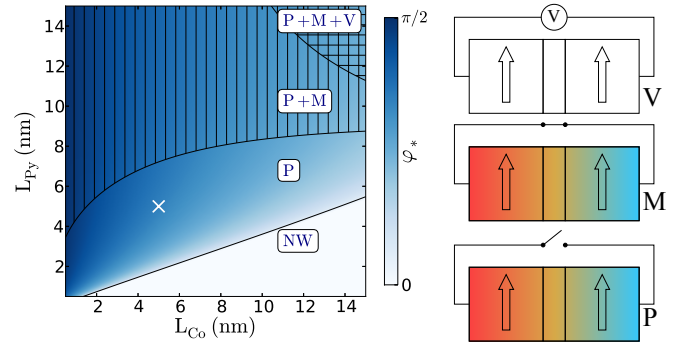


FIG. 2. Left: Waviness angle φ^* of the pure thermal torque τ_P as a function of L_{Co} and L_{Py} . The white cross indicates value $L_{Co} = L_{Py} = 5$ nm corresponding to Fig. 1. The presence of a letter V, M or P in a given region means that the angular dependence of the corresponding torque τ_V , τ_M or τ_P is wavy. NW indicates the region where none of them are wavy. Right: cartoon of our three measurement setups V, M, and P. In M and P a temperature difference is applied across the pillar.

uniaxial anisotropy, the critical torque (per unit angle and per unit surface of the spin valve) needed to destabilize the initial (parallel or anti-parallel) configuration is given by [11, 28], $\partial\tau/\partial\varphi = \alpha M_s L_{Py} B_u$ where B_u is the uniaxial anisotropy field, α the Gilbert damping coefficient and M_s the magnetization. Using $\tau = \tau_P \Delta T$, we obtain the critical value of the temperature gradient ΔT_P needed to get magnetic switching (or STO) as,

$$\Delta T_P = \frac{\alpha M_s B_u L_{Py}}{\partial\tau_P/\partial\varphi} \approx \frac{L_{Py}}{\partial\tau_P/\partial\varphi} \times 1.67 \text{ kJ} \cdot \text{m}^{-3} \cdot \text{rad}^{-1} \quad (12)$$

The numerical value of the right hand side of the previous expression was obtained by simulating the spin-valve $\text{Py}_{24}|\text{Cu}_{10}|\text{Py}_6(\varphi)$ of [29] for which a critical switching current $I_{\text{crit}} = 10^7 \text{ A} \cdot \text{cm}^{-2}$ has been reported. We calculate a corresponding critical torque of the order of $10^{-5} \text{ J} \cdot \text{m}^{-2} \cdot \text{rad}^{-1}$ which allows us to estimate globally the product $\alpha M_s B_u$. Critical currents of the order of $10^7 \text{ A} \cdot \text{cm}^{-2}$ are rather standard values for current driven STT[29–31] and values up to two orders of magnitude smaller have been reported[32], so that the previous expression is a rather conservative estimate.

Fig. 3 shows the critical temperature difference in the mixed (ΔT_M , top row) and pure case ΔT_P , middle row). The corresponding values for the parallel configuration (left column) are very high and are not reasonable for actual devices using the reported values for the Seebeck coefficients (although one should bear in mind that careful tuning of the material/geometrical properties could be use to decrease these values significantly). However, the temperature gradient needed to destabilize the anti-parallel configuration (right panel) is much smaller and should be within experimental grasp (a few tens of

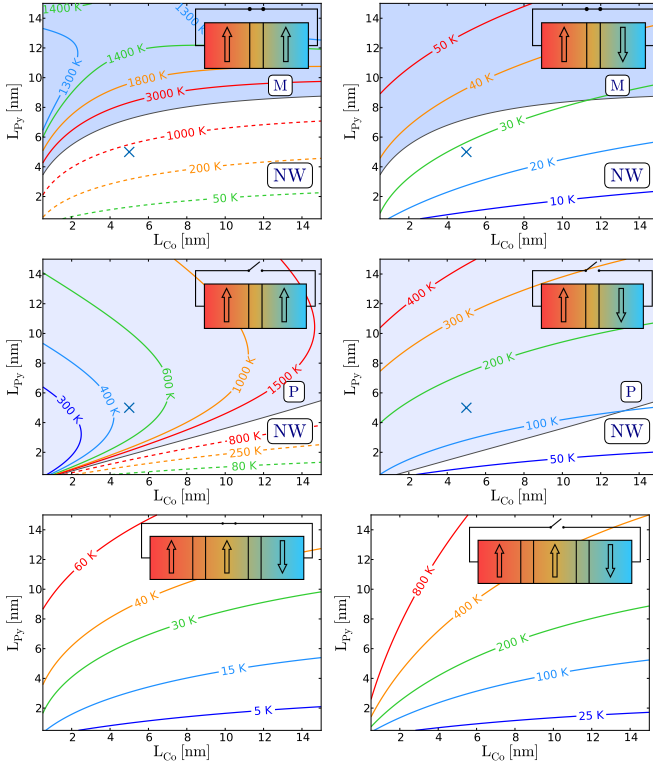


FIG. 3. Temperature difference ΔT needed to achieve the critical torque as a function of L_{Co} and L_{Py} for the mixed (ΔT_M , top row) and pure (ΔT_P , middle row) torques, for a parallel (left column) and antiparallel (right column) configuration, in the $\text{Cu}_{40}|\text{Co}_{L_{Co}}|\text{Cu}_2|\text{Py}_{L_{Py}}(\varphi)|\text{Cu}_{10}$ stack. Dashed lines indicate a negative torque. The blue cross indicates $L_{Co} = L_{Py} = 5$ nm, cf Fig. 1. The background displays the waviness domains of Fig. 2. The bottom row shows the same critical temperature difference for the stack $\text{Cu}_{40}|\text{Co}_{L_{Co}}|\text{Cu}_2|\text{Py}_{L_{Py}}(\varphi)|\text{Cu}_2|\text{Co}_{L_{Co}}|\text{Cu}_{40}$ for the mixed (left) and pure (right) torques.

Kelvin). To further decrease the critical temperature, we consider a slightly different stack (bottom row of Fig. 3) where a third magnetic layer, antiparallel to the first (polarizing) layer has been introduced to enhance the torque. Such an extra layer makes the system perfectly symmetric and therefore makes the waviness behavior disappear. On the other hand, we find a very significant lowering of the critical temperature down to values of a few Kelvin. We find such a low threshold for magnetic reversal to be very encouraging.

Analytical approach: building efficient effective materials. In the absence of spin-flip scattering, ignoring the finite penetration of transverse spins and keeping only the first order terms from the Seebeck/Peltier effect, close analytical expressions can be obtained for our model. A first result is that many collinear materials (or interfaces) put in series can be combined to obtain a unique effective material. After such a procedure our spin valve can be reduced to two effective layers A and B whose magneti-

zations make an angle φ . The effective parameters read,

$$\bar{r} = \sum_i r_i \quad (13)$$

$$\bar{r}\bar{\beta} = \sum_i r_i \beta_i \quad (14)$$

$$\bar{r}(1 - \bar{\beta}^2)/\bar{\mathcal{L}} = \sum_i r_i(1 - \beta_i^2)/\mathcal{L}_i \quad (15)$$

$$\bar{r}(1 - \bar{\beta}^2)\bar{s}/\bar{\mathcal{L}} = \sum_i r_i(1 - \beta_i^2)s_i/\mathcal{L}_i \quad (16)$$

$$\bar{r}(1 - \bar{\beta}^2)\bar{\Delta s}/\bar{\mathcal{L}} = \sum_i r_i(1 - \beta_i^2)\Delta s_i/\mathcal{L}_i \quad (17)$$

where the resistance r_i of a bulk layer (interface) is given by the ratio $2\rho_*L_i/\mathcal{R}_{\text{Sh}}$, where L_i is the thickness of the layer ($2r_b^*/\mathcal{R}_{\text{Sh}}$). These equations can form the basis for engineering the effective parameters and increase the torque of the stack. By placing two of these effective materials A and B in series, we obtain a general description of a spin-valve $F_A|N|F_B(\varphi)$. After some algebra, we obtain the expression of the torque on layer B,

$$\begin{aligned} \tau = & -\frac{F}{2} \sin \varphi \left\{ \left[\beta_A \frac{r_B + 1}{r_B} - \beta_B \cos \varphi \right] (GYeV_b + Sk_B\Delta T) \right. \\ & \left. + \left[\frac{\Delta s_A}{\mathcal{L}_A} (1 - \beta_A^2) \frac{r_B + 1}{r_B} - \frac{\Delta s_B}{\mathcal{L}_B} (1 - \beta_B^2) \cos \varphi \right] Kk_B\Delta T \right\} \end{aligned} \quad (18)$$

where F , G , Y , K and S are expressions involving the various material parameters whose sign do not change when φ varies (see supplementary material for explicit expressions). We have checked Eq. (18) against our numerical simulations and found excellent agreement (see Fig. 1). We find that the current $j^c \propto GYeV_b + Sk_B\Delta T$ so that the open-circuit condition for τ_P is obtained using $GYeV_b + Sk_B\Delta T = 0$. While the expression of Eq. (18) is somewhat cumbersome, the analysis of its angular dependence allows one to obtain simple criteria for the existence of a wavy regime. We find,

$$\cos \varphi_*^V = \frac{\beta_A}{\beta_B} \frac{r_B + 1}{r_B} \quad (19)$$

$$\cos \varphi_*^P = \frac{1 - \beta_A^2}{1 - \beta_B^2} \frac{\mathcal{L}_B}{\mathcal{L}_A} \frac{\Delta s_A}{\Delta s_B} \frac{r_B + 1}{r_B} \quad (20)$$

where the above expressions provide first a criterion for waviness ($|\cos \varphi_*| \leq 1$) and second the value of φ_* for wavy structures. We find that the criterion for waviness in the "pure" thermal case contains two conflicting contributions: in order to obtain a wavy structure one needs the polarization of the resistivity of the free (B) layer to be small while the corresponding Seebeck coefficient is highly spin polarized. As both are not necessarily correlated (the former is related to the polarization of the density of state while the latter to its variation with respect to energy), this leaves much room for material optimization.

Conclusion. We have developed a quantitative theory for spin dependent Seebeck and Peltier effects in magnetic metallic devices. The theory relies entirely on measured material parameters so that its results do not depend on a - always precarious - detailed microscopic modeling. We find that temperature gradient as low as a few degrees should be enough for magnetic switching. Such low temperature gradients could be used in spintronics devices, either alone or to assist current induced switching.

Acknowledgement Funding was provided by the FP7 project STREP MACALO and the consolidator ERC grant MesoQMC.

-
- [1] G. E. W. Bauer, E. Saitoh, and B. J. van Wees, *Nat Mater* **11**, 391 (2012), ISSN 1476-1122.
 - [2] M. Hatami, G. E. W. Bauer, Q. Zhang, and P. J. Kelly, *Phys. Rev. Lett.* **99**, 066603 (2007).
 - [3] X. Jia, K. Xia, and G. E. W. Bauer, *Phys. Rev. Lett.* **107**, 176603 (2011).
 - [4] K. Uchida, S. Takahashi, K. Harii, J. Ieda, W. Koshibae, K. Ando, S. Maekawa, and E. Saitoh, *Nature* **455**, 778 (2008).
 - [5] K. Uchida, T. Ota, K. Harii, S. Takahashi, S. Maekawa, Y. Fujikawa, and E. Saitoh, *Solid State Communications* **150**, 524 (2010).
 - [6] T. Kikkawa, K. Uchida, Y. Shiomi, Z. Qiu, D. Hou, D. Tian, H. Nakayama, X.-F. Jin, and E. Saitoh, *Phys. Rev. Lett.* **110**, 067207 (2013).
 - [7] C. Jia and J. Berakdar, *ArXiv e-prints* (2013), 1310.2331.
 - [8] D. Ralph and M. Stiles, *Journal of Magnetism and Magnetic Materials* (2008).
 - [9] E. B. Myers, D. C. Ralph, J. A. Katine, R. N. Louie, and R. A. Buhrman, *Science* **285**, 867 (1999).
 - [10] J. A. Katine, F. J. Albert, R. A. Buhrman, E. B. Myers, and D. C. Ralph, *Phys. Rev. Lett.* **84**, 3149 (2000).
 - [11] J. C. Slonczewski, *JMMM* **62**, L1 (1996).
 - [12] L. Berger, *Phys. Rev. B* **54**, 9353 (1996).
 - [13] Z. Li and S. Zhang, *Phys. Rev. B* **68**, 024404 (2003).
 - [14] D. Houssameddine, U. Ebels, B. Dieny, K. Garello, J.-P. Michel, B. Delaet, B. Viala, M.-C. Cyrille, J. A. Katine, and D. Mauri, *Phys. Rev. Lett.* **102**, 257202 (2009).
 - [15] O. Boulle, V. Cros, J. Grollier, L. G. Pereira, C. Deranlot, F. Petroff, G. Faini, J. Barnaś, and A. Fert, *Phys. Rev. B* **77**, 174403 (2008).
 - [16] V. S. Rychkov, S. Borlenghi, H. Jaffres, A. Fert, and X. Waintal, *Phys. Rev. Lett.* **103**, 066602 (2009).
 - [17] M. Gmitra and J. Barnaś, *Phys. Rev. B* **79**, 012403 (2009).
 - [18] J. C. Slonczewski, *Phys. Rev. B* **82**, 054403 (2010).
 - [19] F. K. Dejene, J. Flipse, and B. J. van Wees, *Phys. Rev. B* **86**, 024436 (2012).
 - [20] J. Flipse, F. Bakker, A. Slachter, F. K. Dejene, and B. J. van Wees, *Nat Nano* **7**, 166 (2012).
 - [21] X. Waintal, E. B. Myers, P. W. Brouwer, and D. C. Ralph, *Phys. Rev. B* **62**, 12317 (2000).
 - [22] S. Borlenghi, V. Rychkov, C. Petitjean, and X. Waintal, *Phys. Rev. B* **84**, 035412 (2011).
 - [23] T. Valet and A. Fert, *Phys. Rev. B* **48**, 7099 (1993).
 - [24] C. Petitjean, D. Luc, and X. Waintal, *Phys. Rev. Lett.* **109**, 117204 (2012).
 - [25] G. E. W. Bauer, Y. Tserkovnyak, D. Huertas-Hernando, and A. Brataas, *Phys. Rev. B* **67**, 094421 (2003).
 - [26] F. L. Bakker, A. Slachter, J.-P. Adam, and B. J. van Wees, *Phys. Rev. Lett.* **105**, 136601 (2010).
 - [27] A. Slachter, F. L. Bakker, and B. J. van Wees, *Phys. Rev. B* **84**, 174408 (2011).
 - [28] O. Parcollet and X. Waintal, *Phys. Rev. B* **73**, 144420 (2006).
 - [29] M. AlHajDarwish, H. Kurt, S. Urazhdin, A. Fert, R. Loloee, W. P. Pratt, and J. Bass, *Phys. Rev. Lett.* **93**, 157203 (2004).
 - [30] Y. Jiang, T. Nozaki, S. Abe, T. Ochiai, A. Hirohata, N. Tezuka, and K. Inomata, *Nat Mater* **3**, 361 (2004).
 - [31] S. Zhang, P. M. Levy, and A. Fert, *Phys. Rev. Lett.* **88**, 236601 (2002).
 - [32] T. Yang, T. Kimura, and Y. Otani, *Nat Phys* **4**, 851 (2008).

DERIVATION OF THE SPIN TORQUE EXPRESSION FREFEQ:TORQUE

Eq.(18) was derived in the case of a spin-valve $F_A|N|F_B(\varphi)$, under the following assumptions: (i) the spin-valve has no variations along the y and z directions, (ii) spin-flip scattering is neglected, (iii) the transverse spin is absorbed at the Normal-Ferro interface (ℓ_\perp very short), (iv) the Seebeck coefficients s and Δs are only considered at first order and (v) the various layers that make the two effective materials F_A and F_B have a single orientation of their magnetization. The normal spacer is taken to be perfectly transparent without loss of generality as any finite resistance can be incorporated in the effective material F_A or F_B . We note that in the numerics presented in the main text, condition (ii) and (iv) are relaxed which only lead to small corrections to the results.

Within this set of approximations, Eq. (4) to (9) become for each material:

$$-\ell_* \frac{d\mu_c}{dx} = j^c - \beta j_\parallel - s' j^q \quad (\text{SM-21})$$

$$-\ell_* \frac{d\mu_\parallel}{dx} = j_\parallel - \beta j^c - \Delta s' j^q \quad (\text{SM-22})$$

$$-\ell_* \frac{d\theta}{dx} = -s' j^c - \Delta s' j_\parallel + \frac{(1 - \beta^2)}{\mathcal{L}} j^q \quad (\text{SM-23})$$

and the conservation equations are:

$$\frac{dj^c}{dx} = 0 \quad (\text{SM-24})$$

$$\frac{dj^q}{dx} = 0 \quad (\text{SM-25})$$

$$\frac{dj_\parallel}{dx} = 0 \quad (\text{SM-26})$$

with $j_\parallel = \mathbf{j} \cdot \mathbf{m}$, $\mu_\parallel = \boldsymbol{\mu} \cdot \mathbf{m}$, $s' = \frac{1 - \beta^2}{\mathcal{L}} s$ and $\Delta s' = \frac{1 - \beta^2}{\mathcal{L}} \Delta s$

The conservation equations imply that j^c and j^q are constant, and the absence of spin-flip makes j_\parallel piecewise constant. As a consequence, μ_c , θ and μ_\parallel are piecewise linear so that Eq. (SM-21) to Eq. (SM-23) can be easily integrated leading to the effective materials described in Eqs.(13) - (17). The matching of spin accumulation of the a ferromagnet with the normal spacer is described by,

$$n_x j_a^c = \frac{\mathcal{R}_{\text{Sh}}}{4r_*^b} \Delta \mu_c \quad (\text{SM-27})$$

$$n_x j_a = \frac{\mathcal{R}_{\text{Sh}}}{4r_*^b} (\Delta \boldsymbol{\mu} \cdot \mathbf{m}) \mathbf{m} + \varepsilon_a (\mathbf{m} \times \boldsymbol{\mu}_a) \times \mathbf{m} \quad (\text{SM-28})$$

$$n_x j_a^q = \mathcal{L} \frac{\mathcal{R}_{\text{Sh}}}{4r_*^b} \Delta \theta \quad (\text{SM-29})$$

with $n_x = -1$ (+1) for the $F_A|N$ ($N|F_B$) interface, r_*^b the square resistance of the interface, $\Delta X = X_N - X_F$ representing the difference of a quantity between the spacer and the ferromagnetic side, and $\varepsilon_N = -\varepsilon_F = 1$. The subscript a indicates on which side of the interface the quantity are evaluated (N or F).

Taking the limit of a transparent interface translates to $r_*^b \rightarrow 0$. This yields $\Delta \mu_c = 0$, $\Delta \boldsymbol{\mu} \cdot \mathbf{m} = 0$ and $\Delta \theta = 0$. Applying Eq.(SM-28) twice, and eliminating all the variables linked to the spacer provides the matching conditions for the spin currents and accumulations between F_A and F_B . Specifically, denoting $\boldsymbol{\mu}_A$ (resp $\boldsymbol{\mu}_B$) the vector spin accumulation in layer A (resp. B) infinitely close to its interface with the normal spacer. We have $\boldsymbol{\mu}_A = \mu_A \mathbf{m}_A = \mu_A \mathbf{e}_z$, and $\boldsymbol{\mu}_B = \mu_B \mathbf{m}_B = \mu_B (\sin \varphi \mathbf{e}_x + \cos \varphi \mathbf{e}_z)$. Introducing μ_x and μ_z the components of the spin accumulation inside the normal spacer, we get:

$$\mu_z = \mu_{\parallel A} \quad (\text{SM-30})$$

$$\mu_x \sin \varphi + \mu_z \cos \varphi = \mu_{\parallel B} \quad (\text{SM-31})$$

$$j_z = j_{\parallel A} \quad (\text{SM-32})$$

$$j_x \sin \varphi + j_z \cos \varphi = j_{\parallel B} \quad (\text{SM-33})$$

$$j_x = -\mu_x \quad (\text{SM-34})$$

$$j_x \cos \varphi - j_z \sin \varphi = \mu_x \cos \varphi - \mu_z \sin \varphi \quad (\text{SM-35})$$

By eliminating j_x , μ_x , j_z and μ_z , we obtain:

$$\mu_{\parallel A} - j_{\parallel A} = \cos \varphi (\mu_{\parallel B} - j_{\parallel B}) \quad (\text{SM-36})$$

$$\mu_{\parallel B} + j_{\parallel B} = \cos \varphi (\mu_{\parallel A} + j_{\parallel A}) \quad (\text{SM-37})$$

The last set of equations that we need are the boundary conditions at the reservoirs. They read:

$$j^c + \mu_c^L = eV_b \quad (\text{SM-38})$$

$$j^c - \mu_c^R = 0 \quad (\text{SM-39})$$

$$j_{\parallel A} + \mu_\parallel^L = 0 \quad (\text{SM-40})$$

$$j_{\parallel B} - \mu_\parallel^R = 0 \quad (\text{SM-41})$$

$$j^q + \theta^L = k_B \Delta T \quad (\text{SM-42})$$

$$j^q - \theta^R = 0 \quad (\text{SM-43})$$

with $\mu_c^{L/R}$, $\mu_\parallel^{L/R}$, $\theta^{L/R}$ the value of the potential, spin-resolved potential and temperature infinitely close to the left (L) and right (R) reservoir.

Finally, after some algebra, we can obtain the expressions of the currents and potentials:

$$j^c = FG [GYeV_b + Sk_B \Delta T] \quad (\text{SM-44})$$

$$j^q = FG [SeV_b + Kk_B \Delta T] \quad (\text{SM-45})$$

$$j_{\parallel A} = F\gamma_A [GYeV_b + Sk_B \Delta T] + FK\delta_A k_B \Delta T \quad (\text{SM-46})$$

$$j_{\parallel B} = F\gamma_B [GYeV_b + Sk_B \Delta T] + FK\delta_B k_B \Delta T \quad (\text{SM-47})$$

$$\mu_c = 2r_B F \left(\left[\left(1 + \frac{1}{2r_B} \right) G - \beta_B \gamma_B \right] [GYeV_b + Sk_B \Delta T] - [s'_B G + \Delta s'_B \gamma_B] Kk_B \Delta T \right) \quad (\text{SM-48})$$

$$\mu_{\parallel A} = F \left[\beta_A \left(1 + \frac{1}{r_B} \right) - \beta_B \cos \varphi - \gamma_A \right] [GYeV_b + Sk_B \Delta T] + F \left[\Delta s'_A \left(1 + \frac{1}{r_B} \right) - \Delta s'_B \cos \varphi - \delta_A \right] Kk_B \Delta T \quad (\text{SM-49})$$

$$\mu_{\parallel B} = -F \left[\beta_B \left(1 + \frac{1}{r_A} \right) - \beta_A \cos \varphi - \gamma_B \right] [GYeV_b + Sk_B \Delta T] - F \left[\Delta s'_B \left(1 + \frac{1}{r_A} \right) - \Delta s'_A \cos \varphi - \delta_B \right] Kk_B \Delta T \quad (\text{SM-50})$$

$$\theta = 2r_B F \left[\left(\frac{1 - \beta_B^2}{\mathcal{L}_B} + \frac{1}{2r_B} \right) (SeV_b + Kk_B \Delta T) - Y (s'_B G + \Delta s'_B \gamma_B) eV_b \right] \quad (\text{SM-51})$$

with the following notations:

$$G = \frac{1}{2} \left(\sin^2 \varphi + \frac{1}{r_A} + \frac{1}{r_B} + \frac{1}{r_A r_B} \right) \quad (\text{SM-52})$$

$$Y = \left(\frac{1 - \beta_B^2}{\mathcal{L}_B} + \frac{1}{2r_B} \right) \frac{1}{2r_A} + \left(\frac{1 - \beta_A^2}{\mathcal{L}_A} + \frac{1}{2r_A} \right) \frac{1}{2r_B} \quad (\text{SM-53})$$

$$\gamma_i = \left(\frac{1}{2} \sin^2 \varphi + \frac{1}{2r_j} \right) \beta_i + \frac{1}{2r_i} \beta_j \cos \varphi \quad (\text{SM-54})$$

$$\delta_i = \left(\frac{1}{2} \sin^2 \varphi + \frac{1}{2r_j} \right) \Delta s'_i + \frac{1}{2r_i} \Delta s'_j \cos \varphi \quad (\text{SM-55})$$

$$K = \frac{1}{2} \left(\frac{1}{r_A} + \frac{1}{r_B} + \frac{1}{r_A r_B} \right) G - \frac{r_B \beta_B \gamma_B + r_A \beta_A \gamma_A}{2r_A r_B} \quad (\text{SM-56})$$

$$S = \frac{1}{2r_A} (s'_B G + \Delta s'_B \gamma_B) + \frac{1}{2r_B} (s'_A G + \Delta s'_A \gamma_A) \quad (\text{SM-57})$$

$$F = \frac{1}{2r_A} \frac{1}{2r_B} \frac{1}{KGY} \quad (\text{SM-58})$$

The torque on layer B is defined by $\boldsymbol{\tau} = \mathbf{J}_N - \mathbf{J}_B = \frac{2\hbar}{e^2 \mathcal{R}_{\text{Sh}}} (j_x \mathbf{e}_x + j_z \mathbf{e}_z - \mathbf{j}_{\parallel B}) = \frac{2\hbar}{e^2 \mathcal{R}_{\text{Sh}}} \tau \mathbf{e}_1$, where \mathbf{e}_1 is the in-plane normal vector orthogonal to the magnetization of F_B . We obtain,

$$\begin{aligned} \tau &= -\frac{1}{2} \sin \varphi (\mu_{\parallel A} + j_{\parallel A}) \\ &= -\frac{F}{2} \sin \varphi \left\{ \left[\beta_A \left(1 + \frac{1}{r_B} \right) - \beta_B \cos \varphi \right] (GYeV_b + Sk_B \Delta T) \right. \\ &\quad \left. + \left[\frac{\Delta s_A}{\mathcal{L}_A} (1 - \beta_A^2) \left(1 + \frac{1}{r_B} \right) - \frac{\Delta s_B}{\mathcal{L}_B} (1 - \beta_B^2) \cos \varphi \right] Kk_B \Delta T \right\} \end{aligned} \quad (\text{SM-59})$$

with $(i, j) = (A, B)$ or (B, A)

The expression of the waviness angle is, for any applied temperature gradient and/or voltage:

$$\cos \varphi_* = \frac{\beta_A(1 + \frac{1}{r_B})(GYeV_b + Sk_B\Delta T) + \frac{\Delta s_A}{\mathcal{L}_A}(1 - \beta_A^2)(1 + \frac{1}{r_B})Kk_B\Delta T}{\beta_B(GYeV_b + Sk_B\Delta T) + \frac{\Delta s_B}{\mathcal{L}_B}(1 - \beta_B^2)Kk_B\Delta T} \quad (\text{SM-60})$$

MATERIAL PARAMETERS

For the sake of completeness, we provide the parameters used for the numerical simulations. We used $\mathcal{R}_{\text{Sh}} = 2 \text{ f}\Omega \cdot \text{m}^2$, and the values given in the following tables:

Bulk material	ρ_* [$\Omega \cdot \text{nm}$]	β	ℓ_{sf} [nm]	s	Δs	\mathcal{L}
Cu	5	0	500	0.0185	0	$\pi^2/3$
Co	75	0.46	60	-0.25	-0.02	$\pi^2/3$
Py	291	0.76	5.5	-0.21	-0.044	$\pi^2/3$

TABLE I. material parameters for the bulk materials

Interface material	r_b^* [$\text{f}\Omega \cdot \text{m}^2$]	γ	δ	T_{mx}	R_{mx}	\mathcal{L}
Cu Co	0.51	0.77	0	0	0	$\pi^2/3$
Cu Py	0.5	0.7	0	0	0	$\pi^2/3$

TABLE II. material parameters for the interfaces